

RUBBER-PARTICLE-SIZE DEPENDENT STRAIN RATE EFFECTS ON MECHANICAL PROPERTIES AND DEFORMATION BEHAVIOUR OF HIGH-IMPACT POLYSTYRENE

Takashi Kuboki¹, Kiyoshi Takahashi¹, Pean-Yue Ben Jar², Tetsuya Shinmura³

¹ Research Institute for Applied Mechanics, Kyushu University, 6-1 Kasuga-koen, Kasuga-city, Fukuoka 816-8580, Japan

² Department of Mechanical Engineering, University of Alberta, Edmonton, Alberta, T6G2G8, Canada

³ Research & Development Department, Chiba Plant, Denki Kagaku Kogyo Co., Ltd., 6 Goiminamikaigan, Ichihara, Chiba, 290-0045, Japan

ABSTRACT

Mechanical properties and deformation behaviour of two high-impact polystyrenes, named 0.45S and 0.84S that have salami-structured rubber particles of 0.45 μm and 0.84 μm in diameter, respectively, were studied as a function of strain rate ranging from $2.8 \times 10^{-3} \text{ s}^{-1}$ to $1.8 \times 10 \text{ s}^{-1}$. Comparison of fracture energies obtained from force-displacement curves suggested that values for 0.84S were slightly higher than those for 0.45S under strain rates up to $1.6 \times 10^{-1} \text{ s}^{-1}$. However, the difference was significantly increased at the highest strain rate, mainly because the values for 0.84S remarkably increased while those for 0.45S decreased. Transmission electron microscopic observation showed that at the highest strain rate, crazes were generated only from a few rubber particles in 0.45S while many crazes were generated from rubber particles in 0.84S. It is concluded that the fracture energy difference at the highest strain rate was caused by the difference in the number of crazes generated from each of the rubber particles.

KEYWORDS

HIPS, rubber particle size, strain rate, deformation behaviour, craze

INTRODUCTION

Mechanical properties of polymers strongly depend on time and temperature due to their viscoelastic nature of deformation behaviour. In general, brittleness of polymers is known to increase with the increase of the strain rate. However, for high-impact polystyrene (HIPS) Vu-Khanh [1], based on results from three-point bending tests on notched specimens, reported the increase of fracture energy for crack initiation at a loading speed above 1 m/s. We also reported a similar fracture energy increase for un-notched HIPS specimens under a high strain rate [2].

It is yet to be certain if the above toughness increase at the high strain rate is universal for HIPS of different

compositions, as many parameters, such as molecular weight of the matrix, rubber content, rubber particle size, rubber particle structure, and rubber cross-link density, affect the mechanical properties. The most significant factor for HIPS fracture resistance is believed to be the size of the rubber particles, as only HIPS with a certain range of particle size shows the optimum mechanical properties [3-7].

In this paper, effects of the strain rate on mechanical properties for two HIPSs that have different rubber particle size are studied.

EXPERIMENTAL

Materials

Two HIPS materials were used in the study (named 0.45S and 0.84S). Composition of styrene (St) and butadiene (Bd), weight average molecular weight of polystyrene (PS), average size of rubber particles and morphology of rubber particles are given in Table 1. The main difference between the two materials is rubber particle size, 0.45 μm and 0.84 μm for 0.45S and 0.84S, respectively. TEM micrographs showed that particles of salami structure with polystyrene occlusions were well dispersed in the polystyrene matrix for each material.

Mechanical Tests

Mechanical tests were carried out on un-notched tensile specimens using a servo-hydraulic tensile machine for lower strain rates and a falling weight type impact tensile test machine [8] for higher strain rates. Strain was measured using an optical-fibre extensometer [9] constructed in our laboratory [8].

Examination of Deformation Behaviour

Fractured specimens were studied by transmission optical microscopy and transmission electron microscopy (TEM). Regions near the fracture surface were selected for the TEM study. The TEM specimens were firstly stained in the vapour of an OsO_4 solution of 2 weight percent before being sliced by an ultramicrotome equipped with a diamond knife. Hitachi H7100 TEM, operated at 75 kV, was used for the observation.

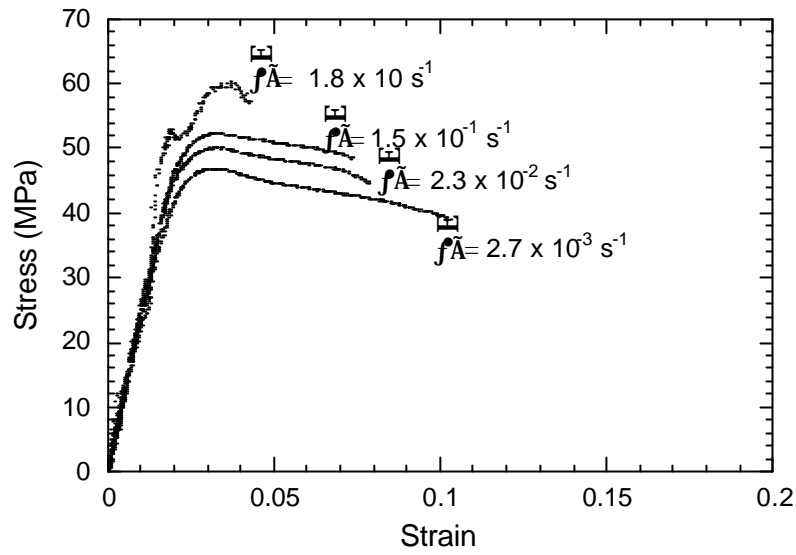
RESULTS AND DISCUSSION

Mechanical Tests

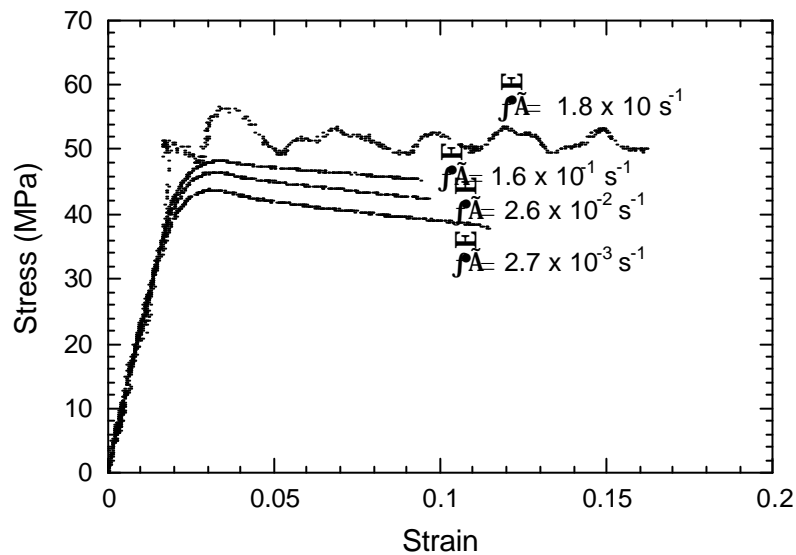
Fig. 1 shows typical stress-strain curves at different strain rates. At the highest strain rate of $1.8 \times 10^{-1} \text{ s}^{-1}$, oscillation was observed in the curves for both 0.45S (Fig.1 (a)) and 0.84S (Fig. 1 (b)). The oscillation is an indication of the dynamic loading effect, due to vibration and stress wave propagation. When the oscillation occurred, the maximum stress was determined based on the “oscillation-centre”, defined as the mean value of the adjacent maximum oscillating stress values. The curves also provide mechanical properties such as Young’s modulus and strain at fracture.

TABLE 1 Characteristics of the HIPSs.

Material	Composition (wt%)		Weight average molecular weight of PS	Average size of rubber particles (μm)	Morphology of a rubber particle
	St	Bd			
0.45S	92	8	239,500	0.45	Salami
0.84S	92	8	225,300	0.84	Salami



(a) 0.45S



(b) 0.84S

Figure 1: Typical stress-strain curves under various strain rates.

Both materials showed that the maximum stress increased with the increase of strain rate. The maximum stress values of 0.45S were always higher than those of 0.84S at all strain rates. Young's modulus of the former was also slightly higher than that of the latter at all strain rates. However, the modulus values showed little change with the increase of the strain rate. For the strain at fracture, 0.45S showed a continuous decrease with the increase of the strain rate; but 0.84S firstly showed the decrease with the increase of the strain rate up to $1.6 \times 10^{-1} \text{ s}^{-1}$, and then a remarkably increase by ca. 61 % with a further increase of the strain rate to $1.8 \times 10 \text{ s}^{-1}$. It should be noted that the fracture strain of 0.84S at the highest strain rate of $1.8 \times 10 \text{ s}^{-1}$ is even higher than that at the lowest strain rate of $2.8 \times 10^{-3} \text{ s}^{-1}$. Comparing the fracture strains at the same strain rate, 0.84S was always higher than 0.45S.

Fig. 2 shows fracture energy as a function of strain rate. Fracture energy was calculated based on the total area under the force-displacement curve. The values of 0.45S continuously decreased with the increase of the strain rate. On the other hand, the values of 0.84S firstly showed a decrease with the increase of the strain rate from $2.8 \times 10^{-3} \text{ s}^{-1}$ to $2.5 \times 10^{-2} \text{ s}^{-1}$; a slight increase with a further increase of the strain rate to $1.6 \times 10^{-1} \text{ s}^{-1}$, and a significant increase by ca. 83 % for a further increase of the strain rate to $1.8 \times 10 \text{ s}^{-1}$. The fracture energy of 0.84S was always higher than that of 0.45S at the same strain rates. The value of 0.84S

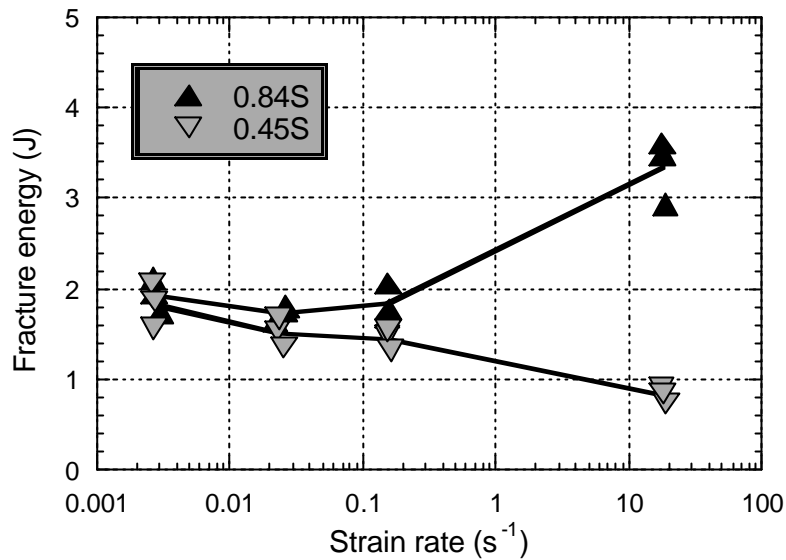


Figure 2: Fracture energy as a function of strain rate.

at the highest strain rate of $1.8 \times 10^{-1} \text{ s}^{-1}$ was the highest obtained from the study. We also noticed that the difference of fracture energy between the two materials increases with the increase of the strain rate, and the difference is remarkable at the highest strain rate of $1.8 \times 10^{-1} \text{ s}^{-1}$.

As the fracture energy variation is dominated by the energy absorption after the point of the maximum stress, as shown in Fig. 1, the fracture energy variation follows very closely the variation of the fracture strain. Therefore, the fracture energy variation is mainly dominated by the strain energy for plastic deformation after the maximum stress point.

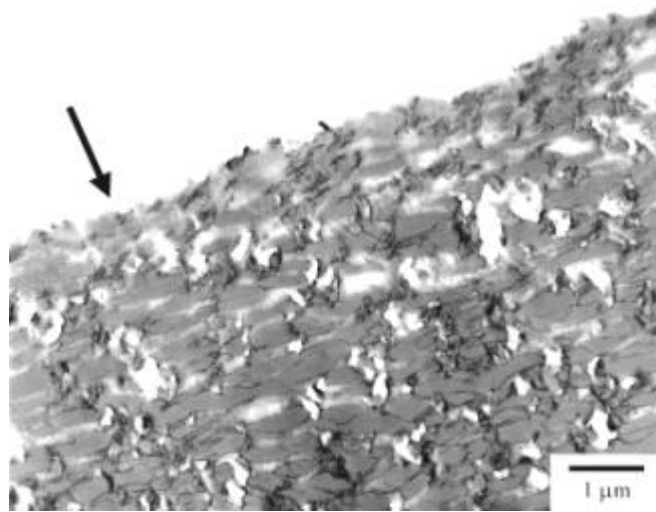
Deformation Behaviour

The deformation mechanisms in the post-fracture specimens were examined in order to facilitate the understanding of the significant difference in the fracture energy between 0.45S and 0.84S at the highest strain rate.

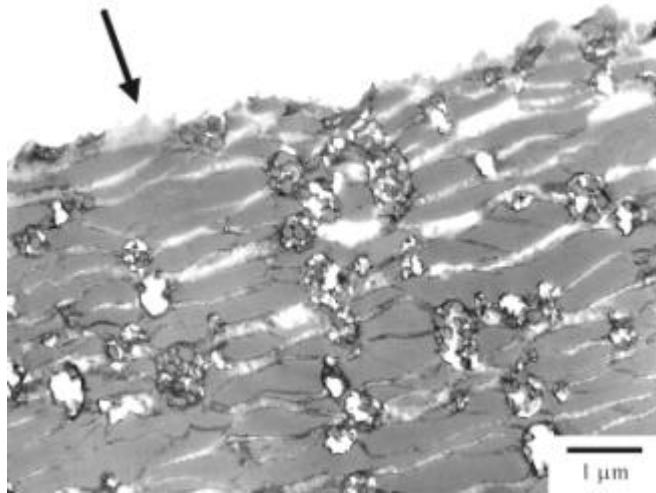
Results of the transmission optical microscopy showed that the size of the stress-whitening zone in 0.84S increased with the increase of the strain rate from $1.6 \times 10^{-1} \text{ s}^{-1}$ to $1.8 \times 10^{-1} \text{ s}^{-1}$, while that in 0.45S decreased. This is consistent with the variation of the fracture energy between the two materials.

Fig. 3 shows TEM micrographs for specimens fractured at the lowest strain rate of $2.8 \times 10^{-3} \text{ s}^{-1}$. Figs. 3 (a) and 3 (b) represent the micrographs of 0.45S and 0.84S, respectively. The micrographs were taken in regions just beneath the fracture surface. An arrow on the micrographs indicates where the fracture surface is. The arrow is also oriented to be parallel to the direction of the tensile loading. Many highly deformed, widely open crazes are shown in both micrographs, in which some of the craze fibrils have already broken down. Such deformation behaviour suggests that crazes have been well developed in the specimens and that fracture was initiated by coalescence of the crazes. Little difference was found in width and number of the crazes in these two micrographs.

Fig. 4 shows TEM micrographs for specimens fractured at the highest strain rate of $1.8 \times 10^{-1} \text{ s}^{-1}$. The micrograph of 0.45S (Fig. 4 (a)) shows that crazes are generated only from some of the rubber particles. On the other hand, the micrograph of 0.84S (Fig. 4 (b)) shows many crazes being generated from each rubber particle. There is a remarkable difference between 0.45S and 0.84S in the number of crazes. Compared to the micrographs from specimens tested at the lowest strain rate, Fig. 3, the number of crazes in Fig. 4 (a) has largely decreased with the increase of the strain rate, while that in Fig. 4 (b) has significantly increased.



(a) 0.45S



(b) 0.84S

Figure 3: TEM micrographs for specimens fractured at the lowest strain rate of $2.8 \times 10^{-3} \text{ s}^{-1}$.

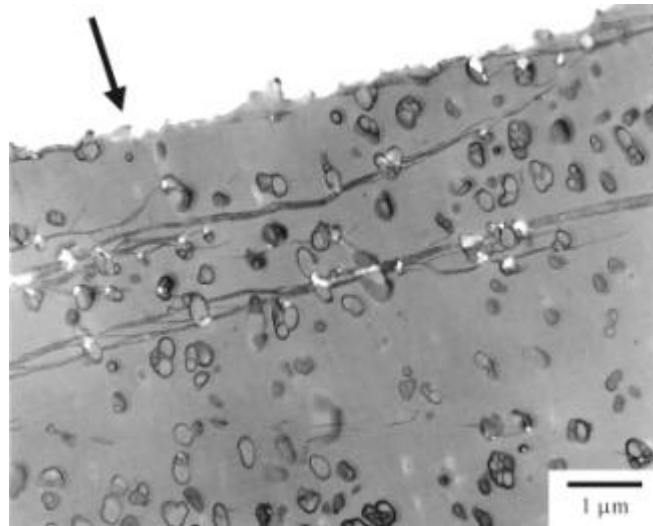
TEM observation showed that crazing was the dominant deformation mechanism in all specimens. At the lowest strain rate, there was no significant difference in the width and number of crazes between the two HIPSs. However, at the highest strain rate, a small number of crazes occurred in the 0.45S and were generated only from a few rubber particles; while many more crazes were generated in the 0.84S and were found from every rubber particle in the micrograph. Therefore, the difference in number of crazes has caused the significant difference in the fracture energy at the highest strain rate.

CONCLUSIONS

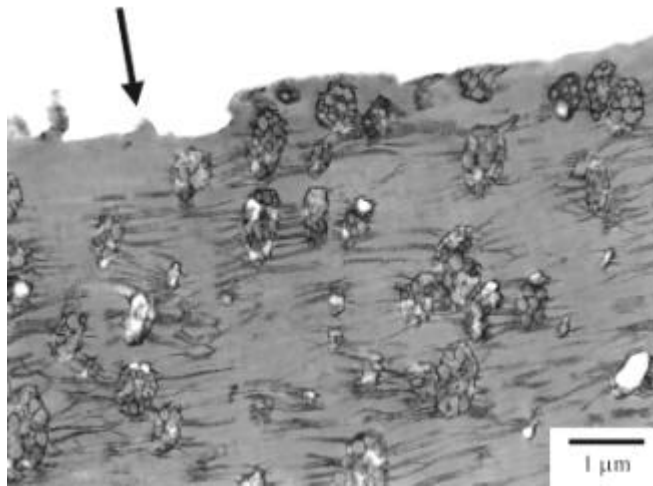
It is concluded that the particle size has strongly affected the fracture energy of the HIPS, especially at the highest strain rate. This is mainly because at the highest strain rate, the rubber particle size has affected the number of crazes generated from each rubber particle.

ACKNOWLEDGEMENT

The authors would like to thank Mr. Mada in Kyushu University and Dr. S. Stowe in the Electron Microscope Unit, The Australian National University for assistance with mechanical tests and transmission



(a) 0.45S



(b) 0.84S

Figure 4: TEM micrographs for specimens fractured at the highest strain rate of $1.8 \times 10^{-1} \text{ s}^{-1}$.

electron microscopy, respectively. Kuboki would also like to acknowledge financial support from Targeted Institutional Links Program (administered by DETYA, Australia) and Japan Society for the Promotion of Science for the scholarship support.

REFERENCES

1. Vu-Khanh, T. (1998) *Theoret. Appl. Fract. Mech.* 29, 75.
2. Kuboki, T., Jar, P.-Y. B., Takahashi, K. and Shinmura, T. (2000). *11th International Conference on Deformation and Fracture of Polymers*, Cambridge, 429.
3. Moore, J.D. (1971) *Polymer* 12, 478.
4. Silberberg, J. and Han, C.D. (1978) *J. Appl. Polym. Sci.* 22, 599.
5. Bucknall, C.B., Davies, P and Partridge, I.K. (1987) *J. Mater. Sci.* 22, 1341.
6. Cook, D.G., Rudin, A. and Plumtree, A. (1993) *J. Appl. Polym. Sci.* 48, 75.
7. Dađli, G., Argon, A.S. and Cohen, R.E. (1995) *Polymer* 36, 2173.
8. Takahashi, K., Mada, T. and Beguelin, Ph. (1998) *Trans. Jpn. Soc. Mech. Eng.* A64, 2975 (in Japanese).
9. Beguelin, Ph., Barbezat, M. and Kausch, H. H. (1991) *J. Physique* III 1, 1867.